ISSN 1110-0354
Bull. Nat. Inst. of Oceangr. & Fish., A.R.E., 2002. Vol. (28): 453 - 465

NUMERICAL COMPUTATIONS OF 1303 TSUNAMIGENIC PROPAGATION TOWARDS ALEXANDRIA, EGYPTIAN COASTS

BY

*A. Z. HAMOUDA**

** Marine Geology and Geophysical Department, National Institute of Oceanography and Fisheries, Kayet Bey, Alexandria, Egypt.*

Keywords: Tsunami, Tsunamigenic, Alexandria, subduction zone, Nile Delta

ABSTRACT

Numerical model is carried out to forecast the probable tsunami behavior for future eruption of Eastern Mediterranean Ridge, and its effect on Alexandria, Egypt. On the 8th of August 1303 a Major earthquake of magnitude about 8 that caused a large tsunami, killing many people around Alexandria and ships were carried over buildings and settled on land.

Calculations were done with an initial condition of continuous water flow normal to the shore line. This case of Tsunamigenic was examined to study the effect of location, direction, travel time and height towards the Egyptian Coast. Computed tsunami features such as travel times and height distribution patterns are shown to be useful for the evaluation of any future tsunami hazard.

INTRODUCTION

At least two big tsunami disasters affecting the Nile Delta and Alexandria have been reported since ancient times. These disasters happened on 21 July 365 and 8 August 1303 respectively (within magnitude about 8). These two earthquakes have similar effects on Alexandria, the Delta of Egypt and the surrounding area in the Eastern Mediterranean. The data for the present analysis are mostly collected from the World Wide Tsunami in the Natural Geophysical Data Center and the Ambraseys et al (1995).

The present paper aims to answer what was the Tsunami mechanism of the 8 August 1303 with magnitude about 8. Also, computed tsunami features such as travel times and height distribution patterns are to be considered to evaluate future tsunami hazard.

DISASTER OF 1303 TSUNAMIGENIC

Old documents describing the 1303 Tsunami earthquake damage, were concentrating on frightening effects of that exceptional seismic sea-wave which struck many localities in the Mediterranean basin. It has been suggested that this extensive sea-wave was caused by an earthquake having its epicenter near the island of Crete. Houses were broken, destroyed and washed away due to buoyancy, drag force, impacts of water and floating materials. In addition to loss of human lives and houses, several kinds of disasters caused by tsunamis in the past were summarized (Ambraseys et al., 1995 and Papazachos,1990).

Shortly after the second light in Alexandria, preceded by several heavy thunder and lightning, the whole stability of the earth was shaken. Huge masses of water flowed back when least expected, and overwhelmed and killed many thousands of people. After subsidence of fury of the waves, some ships were seen to have been destroyed by the rapid whirlpools created by the retreating waters, and the dead bodies from the ships wrecked floated face up or down. Some great ships were hurled by the fury of the waves onto roof tops, and others were thrown up to two miles from the shore.

TECTONICS

Papazachos (1990) noted that the Hellenic arc has a large majority of the earthquake foci lying close to it. Also, the existence of extensional zones close to zones of thrusting in the Eastern Mediterranean area shows its tectonic complexity, Fig. 1.

Papazachos and Comninakis (1971) suggested that the subducted African lithospheric plate is about 90 km thick, which is the approximate thickness of the layers above the top of the low shear-wave velocity layer. The boundary of the zone of South East Crete constitutes the continuation of underthrusting of African lithosphere under the Eurasian Lithosphere south Turkey. This zone includes the pattern of seismicity that hits the outermost part of the subduction, Fig.1. Although this pattern of seismicity is far from the subduction, it is parallel it. So, the seismicity in the subduction zone present beneath Crete is characterized by earthquakes of large magnitudes that have history of affecting Egypt (Maamoun et al., 1984).

The geophysical data confirm the structure, and give clues on the possibility of obtaining useful information as the mean dip and the length of the descending lithospheric plate (Makris and Wang, 1994). The dipping of the seismic zone is clear, but foci of considerable depth are found under the Hellenic trench as if part of the Lithosphere is steeply dipping under the trench, Fig. 2.

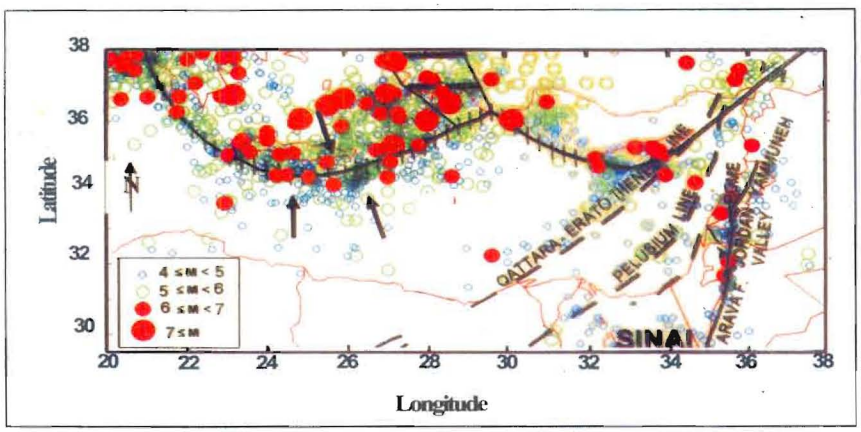

Fig. 1. Earthquake activity and regional tectonics in the Eastern Mediterranean after Riad et al., 1996.

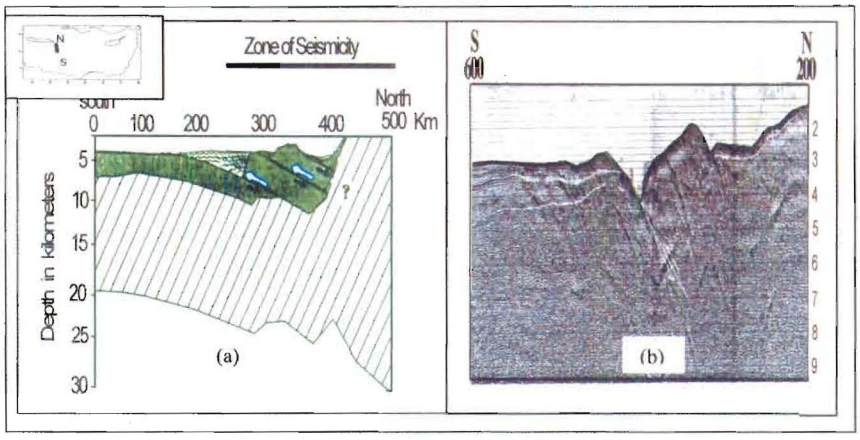

Fig.2: (a) Hypothetical model, showing mechanism of crustal shortening in the Eastern Mediterranean (from Rabinowitz and Ryan,1970). (b) Example of seismic reflection line south of Crete Island. It shows the probable trench zone between the African and European Plates (from Finetti, and Morelli, 1973).

BATHYMETRIC

Fig. (3) represents the bathymetric contour map of the Eastern Mediterranean, the map is modified from the bathymetric contour map of Krasheninnikov and Hall (1994), and a digital bathymetric data obtained from the Natural Geophysical data Center (USA). The Eastern Mediterranean Sea is dominated by an elongated NE-SW trending depression known as the Herodotus Abyssal Plain. South to the Hellenic arc an "external trench" forming a discontinuous series of small bathyal plains up to (3800 to 4000m) included in basins of complicated topography. The Nile cone is characterized by very gentle slope, but the western side has a slightly steep slope.

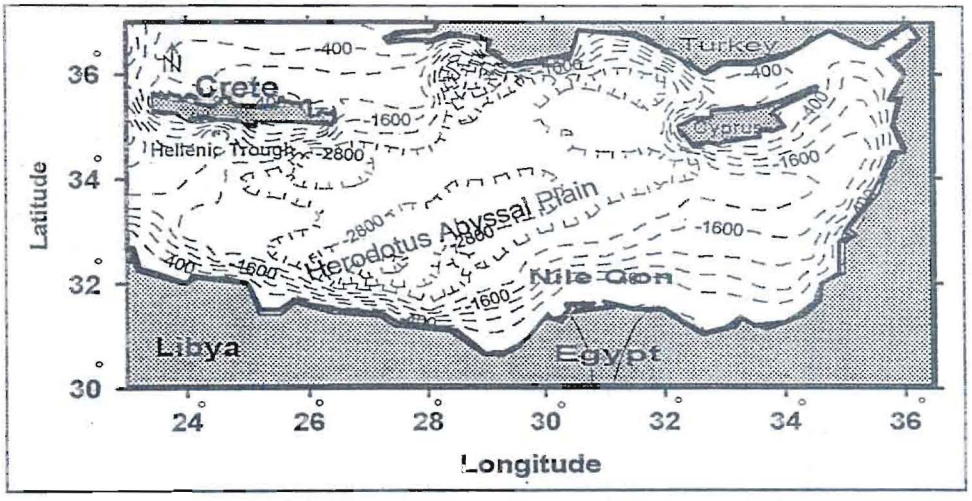

Fig. 3. Modified Bathymetric map of the Eastern Mediterranean Sea (grid 5x5 km) from Makris and Wang (1994) and digital data from Natural Geophysical Data Center.

METHOD

In recent years, numerical simulations have been developed and used to compute the behavior of tsunamis in shallow water and on land. The results of these numerical computations are often referred to in practical designs of defense works against tsunamis. So, there have been many numerical studies of tsunamis such as: Aida (1974 and 1984), Iwasaki and Mano (1979), Abe et al. 1990 and Shuto et al. (1990). Most of them aimed to reproduce historical tsunamis, for which data such as run-up heights, in undated areas and fault models are of little reliance. Aida (1975 and 1984) made such computations for 1792 Unzenand and 1741 Oshima tsunamis to compare with distribution pattern of run up heights estimated from old documents. Abe et al. (1990) carried out the field investigation of the height of Sanriku earthquake tsunami (A.D.869) on the basis of archaeological view and sedimentologic examination.

In the present work, the simulation based on a set of equations of motion and continuity for linear long waves was solved by a leap-frog method in a finite-difference scheme. The present computation uses the linear long wave theory which does not include the physical dispersion term. The linear long wave assumption is valid when the source size is much larger than water depths this is applied in the deep water of the Mediterranean Sea. The linear long-wave theory is applied to the study sea area 200 km long and 250 km wide along the northern cost of Egypt, Fig. 4. Entering shallow water and approaching the shore, a tsunami increase in height, steepness, and curvature of water surface. Equations change according to the order of approximation required to describe it: the linear long-wave and the shallow water theories. In marine area of water depth deeper than 50 m, the linear long-wave theory gives satisfactory results according to the standard deviation and correlation coefficient. As water depth decreases, the equations should be switched to the shallow-water theory with bottom friction, according to Shuto (1991a and b). The numerical calculation is done by using Fortran IV program, the leap-frog scheme, grid points are alternatively located for velocity and water level. The numerical simulation assumes that the water level of the previous cell equals the bottom height of the next landward cell. If the water level is higher than the latter, the water may flow into the landward cell.

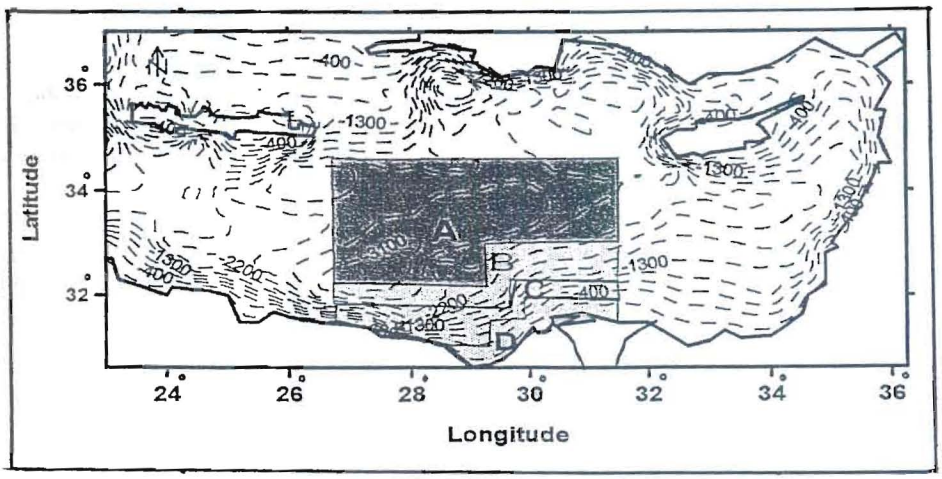

Fig. 4. Adopted grid system for the computation area (grid size: A= 8000 m, B= 4000 m, C= 1000 m and D= 500 m).

Fig. (4) shows the distribution of grid size required for the resolution N=20 based upon Linear long waves of period of 5 minutes. It can be divided into four areas (A, B, C, and D). Each area has uniform grid size intervals (8, 4, 1, 0.5 km, respectively).

FAULT PARAMETERS

Fault mechanism and fault parameters were determined from seismic data collected not only locally but also world-widely and supported by the seismological data. In addition, the author numerical simulation input the data of the model fault parameters in the study area, Fig.2. It is collected from recent seismic data, which has a length is 60 km, width 30 km, depth 3 km dip directions N10 W and dip angle 25°. An immediate conclusion is that the fault dips slightly northward. Since the source was large compared with the water depth, the bottom vertical displacement gave the vertical displacement of the free surface. The vertical displacement of sea bottom at the source area in this model is calculated according to the theory of Mansinha and Smylie (1971). The major result is that a maximum vertical displacement of about 4 m height is obtained at the southern side of the source at the central part, corresponding to the fault which dips northward. Then, the present method of source model, based upon seismic data, can be applied to establish the initial tsunami profile to a first–order approximation but it does not give a full detail explanation of the tsunami.

RESULTS AND DISCUSSION

1. Time arrival

The result of the model calculation is represented by Figs. 5 and 6. Fig.5 shows an animation of the sequence propagation tsunami which generated from the source. If the colors are assigned to particular values of the water surface elevation, an animation becomes easier to be understood. This figure shows the propagating tsunami at 10, 20. 40 minute intervals after the avalanche impact. According to the Aida Model-19 (1984) the crest of tsunami is not at the northern side of the fault plane but at the southern side towards to the Egyptian coast. In order to satisfy this condition, the fault might be considered to dip northward. So, the maximum upheaval at the southern side is corresponding to the northward dip. The tsunami wave propagates faster in deeper water and reaches the opposite shore across the Alexandria in about 40 mints from the source. Generally, the tsunami amplitude decreases with distance from the source and increase again when the wave reaches the shorelines. As expected, tsunamis generated at the interior of the Alexandria bay can be larger than that from source.

Fig. (6) shows the travel time as contours of 2 minuets interval, indicating the maxima of the tsunami first wave. It is clearly recognized that the sea bottom works as lenses and concentrates the tsunami towards Alexandria bay. The tsunami travels slowly where the water depth is relatively shallow. However, the tsunami travels faster in deep water but in the front of Delta will be slower. Thus the wave front may be distorted by the local features of sea bottom topographies.

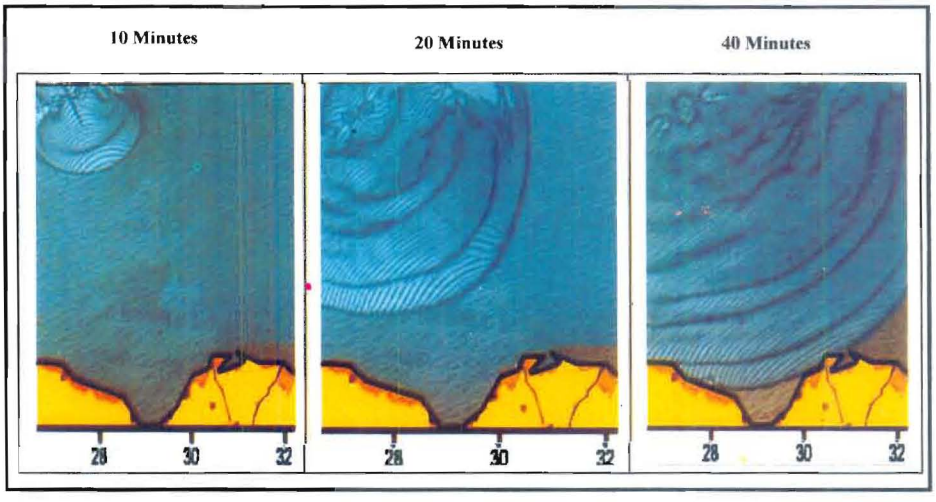

Fig. 5: The propagating tsunami generated from the source towards the Egyptian coast.

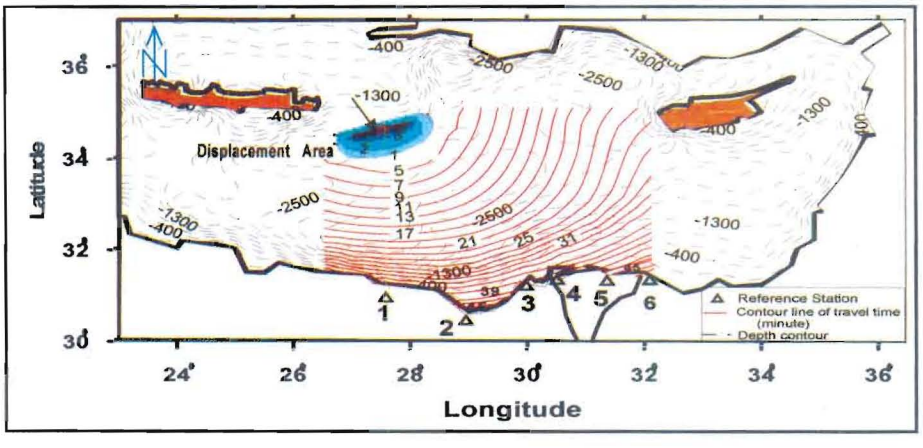

Fig. 6: Computed travel time of the tsunami first wave.

Fig. (6) shows the first tsunami wave arrives at different reference localities in the study area along the Egyptian Coast at different time. The computed arrival times of the first wave are about 37, 47, 40, 37, 45 and 49 minutes at the six localities 1, 2, 3, 4, 5 and 6 respectively. There is a time period of the first tsunami wave arrives in between these references localities 1 and 6 about 12 minuets. This difference related to the shape of the shore line and the sea bottom topography along the Egyptian Coast.

2. Run up height

Abe (1981) introduces an idea that, the height should reach a limiting value within a distance Ro from the source origin, where Ro is taken as the radius of a circular fault. He derived the equation as:

$$\text{Log } Hr = 0.5\ Mw - 3.3 \div C \qquad \ldots\ldots\ldots\ldots \qquad (1)$$

Where Hr is the limiting tsunami height and Mw is the moment magnitude of the earthquake.

Abe (1985) also estimated the height of the regional tsunami at a particular site as:

$$\text{Log } H_t = Mw - \text{Log } R - 5.35 + C \qquad \ldots\ldots\ldots\ldots \qquad (2)$$

Where H_t is tsunami height, R is distance (km), C= 0.0 for tsunamis in the Pacific Ocean and C = 0.2 in the Japanese sea, and Mw is the moment magnitude of the earthquake. This equation gives an unreasonably large estimate of tsunami height near the source.

One of the problems in tsunami computations on land is the boundary condition at the wave front. Water is run up on dry land and run down to leave a dry bed. Even when there is no breaking at the wavefront, the movement of water on the slope can not be easily expressed. There are several methods to overcome this difficulty. According to the method of Iwasaki and Mano (1979), assume that the line connecting the water level and the bottom height gives the surface slope to the first–order approximation. The run–up height computed with the theoretical solution within an accuracy of 5% range.

Waveform and height prediction could be made at any site in the calculation area. Computed tsunami waveforms at reference locations from the source located in Fig. (6) are shown in Fig. (7). The distribution of the maximum tsunami heights from impact is represented during 60 minuets. The travel times and the height distribution patterns presented here can be used to prepare for future tsunamis along the Egyptian Coast.

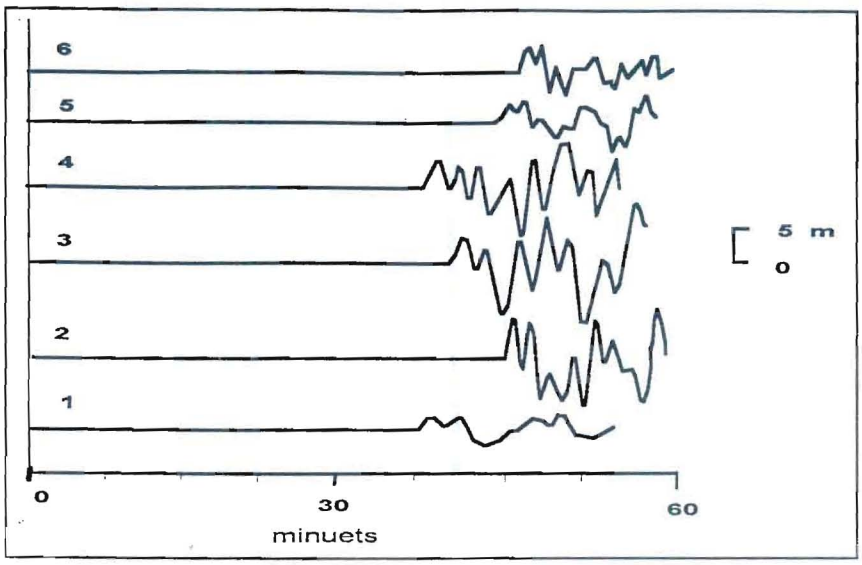

Fig. 7. Computed tsunami wave forms at the reference locations.

The maximum computed run up height of about 9 meters is found in Alexandria on the Egyptian coast at location no. 3. Also, the minimum estimated run up height about 2 meters in the Western Egyptian Coast is at location no. 1. The bottom slop in the front of Delta (Nile Cone) is very gentle as 1/150 to 1/250. Around the point of the maximum run-up, extremely high run-up heights were found to distribute along the beach of slightly smooth shoreline. The sea bottom topography is one of possible causes for high run-up heights for the present tsunami, otherwise it is impossible to explain this concentration of the tsunami. The 1303 tsunami waves might have been amplified by the local topography.

3. Energy Flux

In order to understand the Hellenic arc ridge for tsunami propagation, a numerical simulation was carried out for a hypothetical Eastern Mediterranean bathymetry. The hypothetical bathymetry was obtained under the assumption that the water depths of the south Hellenic arc ridge system are about 3000 m which are almost the same as the depths around this system. Here according to the Koshimura et al, (2001), the maximum energy flux is defined as:

$$E_{max} = \{\rho\, g\, (\Delta x)^2\, (\acute{\eta}_m)^2 / 2\}.\ \sqrt{gh} \qquad \ldots\ldots\ldots\ldots \qquad (3)$$

Where ρ is the water density, Δx is the horizontal grid size, $\acute{\eta}_m$ is the maximum water level at each grid, and h is the water depth. The energy flux distribution starts along the Hellenic arc ridge and transmitted along the ridge towards Alexandria, Fig. 8. This transmission may be one of the causes of relatively high tsunami recorded in Alexandria. The strike direction may affect the propagation direction of tsunami energy which is normal to the long axis of the tsunami source.

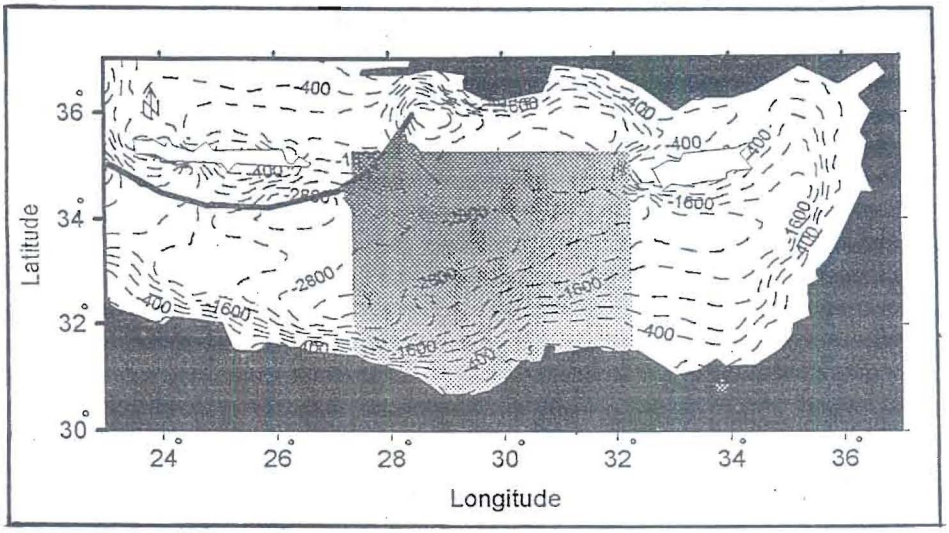

Fig. 8. Computed maximum energy flux distribution with actual sea bottom topography.

4. Tsunami Magnitude and Intensity

This relationship evidently connects the local strength (tsunami intensity) and the total energy (tsunami magnitude) along the distance to the observation station. It is a common rule that the tsunami magnitude is proportional to the earthquake magnitude. A similar consideration by Hatori (1986) to the following equation to express the Imamura-Iida scale of tsunami magnitude by the following equation:

$$M = 2.7 \text{ Log } H + 2.7 \text{ Log } W - 4.3. \quad \ldots\ldots\ldots\ldots \quad (4)$$

Where H is the height of a tsunami above the mean sea level in meters at a given location and W is the shortest travel distance in kilometers from the epicenter to the location (ranging from 20 km to 2,000 km) where the data is obtained. The calculated tsunami magnitude of the 1303 earthquake is 5.

Tsunami intensity is defined as the logarithm of the local tsunami height to the base two, Soloviev (1970). According to Shuto (1991a and 1997) define tsunami intensity with the equivalent disasters, the tsunami intensity is 3 which equivalent to the tsunami height 9 m which computed in Alexandria.

CONCLUSIONS

Numerical simulations with simple source models were presented to examine the probable tsunami from Hellenic arc ridge of the Eastern Mediterranean. Although the probability that would cause such destruction is low, it is easily to understand that the resulted travel time and height distribution patterns are useful to evaluate the essential tsunami hazard towards Nile Delta and Alexandria.

An earthquake and the accompanied tsunami are generated at the same time, but the two phenomena propagate with different speeds. The earthquake arrives at the Egyptian Coast within about 30 second while the tsunami arrives within 35 to 45 minutes. These may be used as one way of predictions which give planners and idea of the best roads for people to take away from the beach (coastal road along the Alex.) if a tsunami happens in the future. The cause of a tsunami is the displacement of sea bottom which is frequently accompanied by an earthquake of great magnitude. Oscillation of ground caused by a tsunamigenic earthquake is generally strong and continues long.

It is emphasized that the generation mechanism of the 1303 tsunami is not simple and is not yet clarified in spite of the rich detailed seismic data. The greatest difficulty is due to the lack of accurate and reliable tsunami records.

To investigate the old tsunamis for which neither tide gage data nor old documents are available, geological observations may provide some useful information not only for the sources but also for the wave heights. In such a work, it is important to identify the hazard which could occur if this tsunami transmitted from Crete towards the coast of Egypt in order to mitigate this hazard. The computed results need verification from tide gauge stations when the future tsunami propagates. Instrumental or empirical observation of tsunami-related phenomena will help to know the approach of a tsunami.

Natural disaster is an interaction between natural forces and human beings. When the social conditions are changed, kind and degree of damage may change. Therefore, we have to acknowledge that the present result is not universal and invariable, but only gives an estimate of expected damages.

ACKNOWLEDGEMENTS

I should like to thanks Prof. Dr. Shuto, Iwate Prefectural University, for their valuable suggestions and discussions and great thanks to for his continuous help. I am grateful to Prof. Dr. Nikhily at Alexandria University, who reviewed the manuscript and for his valuable suggestions and discussions.

REFERENCES

Abe, K., 1985. Quantification of major earthquake tsunamis of the Japan Sea. Phys. Earth Planet. Inter.,38: 214-223.

Abe, K., 1981. Physical size of Tsunamigenic earthquakes of the northwestern Pacific. Phys. Earth Planet. Inter., 27: 194-205.

Abe, H., Sugeno, Y. and Chigama, A., 1990. Estimation of the height of the Sanriku Jogan 11 Earthquake-Tsunami (A.D. 869) in Sendai Plain, Zishin, Vol. 43, pp.513-525.

Aida, I., 1984. An Estimate of Tsunamis Generated by volcanic Eruptions- the 1741 Eruption of Oshima-Ohshima, Hokkaido, Bull. Earthq. Res. Inst., Vol. 59, pp.519-531.

Aida, I., 1975. Numerical Experiments of the Tsunami Associated with the Collapse of Mt. Mayuyama in 1792, Zishin, Vol. 28, pp. 449-460.

Aida, I., 1974. Numerical Computation of a Tsunami Based on a Fault Origin Model of an Earthquake, Zishin, Vol.27, pp. 141-154.

Ambraseys, N. N., Melville C. P, and Adams R. D., 1995. The Seismicity of Egypt, Arabia and the Red Sea a historical Review.

Ambraseys, N. N., 1962. Data for the investigation of the seismic sea-waves in the Eastern Mediterranean, Bull. Seism. Soc. America, 52, 895-913.

Finetti, I., and Morelli, C., 1973. Geophysical exploration of the Mediterranean Sea. Boll. Geofis. Teor. Appl. 15,60.

Hatori, T., 1986. Classification of tsunami magnitude scale, Bull. Earthq. Inst. 61, 503-515.

Iwasaki, T., and Mano, A., 1979. Two-dimensional numerical simulation of tsunami run-ups in the Eulerian description, Proc. 26th Conf. Coastal Eng., JSCE, 70-74.

Krasheninnikov, V., A., and Hall, J, K., 1994. Geological structure of the Northeastern Mediterranean. Pyzhevsky, 109017 Moscow,Russia..

Koshimura, S, I., Imamura, F. and Shuto, N., 2001. Kluwer Academic Puublisher, natural Hazard. 213-229.

Mansinha, L. and Smylie, D. E., 1971. The displacement fields of inclined faults, Bull. Seis. Soc. America, Vol.61, 1433-1440.

Makris, J., and Wang., J. 1994. Bouguer gravity anomalies of the Eastern Mediterranean Sea. Unv. Hamburg. Bundestrass 44, 20146.

Maamoun, M., Megehed, A., and Allam, A., 1984. Seismicity of Egypt. Institute of Astronomy andGeophysics 4.

Papazachos, B. C., 1990. Seismicity of the Agean and surrounding area. Tectonics 178, 287-308.

Papazachos, B., C., and Comninakis, P., E., 1971. Tectonic stress field and seismic fauylting in the area of Greece. Tectonophysics, 7, 3,231-255.

Rabinwitz, P. D., and Ryan, W.B. F, 1970. Gravity anomalies and crustal shortening in the eastern Mediterranean. Tectonophysics, 10, 585-608.

Riad, S., M. Ghalib, M. A. El Difrawy and M., Gamal 1996. Probabilistic seismic hazard assessment in Egypt. First Annual Meeting of The IGCP Project 382, Cairo.1-42.

Shuto, N., 1997. A natural warning of Tsunami arrival, Prespective on Tsunami Hazard Reduction, 157-173..

Shuto, N., 1991a. Tsunami intensity and disasters, Tsunamis in the World, Kluwer Academic Publishers, 197-216.

Shuto, N., 1991b. Numerical simulation of Tsunamis- Its present and Near Future. Natural Hazards, 171-191.

Shuto, N., Goto, G,and Imamura, F., 1990. Numerical simulation as a means of warning for near-field tsunami, Coastal Engineering in Japan, Vol. 33, 173-93.

Soloviev, S. L., 1970. Recurrence of tsunamis in the Pacific, in W. M. Adams (ed.), Tsunamis in the Pacific Ocean, East-West Center Press, Honolulu, 149-163.